

Exploring Models with Modular Symmetry in Neutrino Oscillation Experiments

Priya Mishra,^{1,*} Mitesh Kumar Behera,^{2,†} Papia Panda,^{1,‡} Monojit Ghosh,^{3,§} and Rukmani Mohanta^{1,¶}

¹*School of Physics, University of Hyderabad, Hyderabad - 500046, India*

²*Department of Physics, Faculty of Science,
Chulalongkorn University, Bangkok-10330, Thailand*

³*Center of Excellence for Advanced Materials and Sensing Devices,
Ruder Bošković Institute, 10000 Zagreb, Croatia*

Abstract

Our study aims to investigate the viability of neutrino mass models that arise from discrete non-Abelian modular symmetry groups, i.e., Γ_N with $(N = 1, 2, 3, \dots)$ in the future neutrino experiments T2HK, DUNE, and JUNO. Modular symmetry reduces the usage of flavon fields compared to the conventional discrete flavor symmetry models. Theories based on modular symmetries predict the values of leptonic mixing parameters, and therefore, these models can be tested in future neutrino experiments. In this study, we consider three models based on the A_4 modular symmetry, i.e., Model-A, B, and C such a way that they predict different values of the oscillation parameters but still allowed with respect to the current data. In the future, it is expected that T2HK, DUNE, and JUNO will measure the neutrino oscillation parameters very precisely, and therefore, some of these models can be excluded in the future by these experiments. We have estimated the prediction of these models numerically and then used them as input to scrutinize these models in the neutrino experiments. Assuming the future best-fit values of θ_{23} and δ_{CP} remain the same as the current one, our results show that at 5σ C.L, Model-A can be excluded by T2HK whereas Model-B can be excluded by both T2HK and DUNE. Model-C cannot be excluded by T2HK and DUNE at 5σ C.L. Further; our results show that JUNO alone can exclude Model-B at an extremely high confidence level if the future best-fit of θ_{12} remains at the current-one. We have also identified the region in the θ_{23} - δ_{CP} parameter space, for which Model-A cannot be separated from Model-B in T2HK and DUNE.

* mishpriya99@gmail.com

† miteshbehera1304@gmail.com

‡ ppapia93@gmail.com

§ mghosh@irb.hr

¶ rmisp@uohyd.ac.in

I. INTRODUCTION

The Standard Model (SM) of elementary particles and their interactions suggests that quarks and leptons exist in three generations or families. However, the prevailing reason behind this and the hierarchical nature of fermion masses still remains a mystifying puzzle in particle physics. Additionally, the differences in the mixing patterns between quarks and leptons and whether they have any underlying principles are not yet understood, and together these issues make up the “flavor problem”. One possible explanation for the mixing patterns in the lepton sector is non-Abelian discrete flavor symmetries, which have been extensively studied in the past few decades. However, the small mixing structure in the quark sector does not seem to support non-Abelian discrete symmetries, and attempts to explain both sectors with discrete flavor symmetries are rather challenging. In this article, we will focus only on the lepton sector and try to see if we can probe such models with the neutrino oscillation experiments rather than attempting to address the unified solution to the flavor problem. The discrete symmetry approach to lepton flavor has two main features: (i) it predicts certain values of the neutrino oscillation parameters, and (ii) it establishes algebraic relationships between some of the mixing parameters. These relationships are known as lepton (or neutrino) mixing sum rules and have been illustrated in various references [1, 2]. However, in this article, we try to elucidate the theoretical frameworks based on A_4 modular discrete symmetry group utilizing certain seesaw mechanisms. The most popular seesaw mechanisms used to generate the light neutrino masses as well as definite flavor structure in the neutrino sector are: type-I [3–6], which incorporates three singlet right-handed heavy neutrinos, type-II, with the inclusion of a scalar triplet [7–12], and type-III [13–18], where a fermion triplet is added to the SM particle content. In these approaches, the masses of the new heavy particles are rather heavy and are beyond the access of the present or future experiments. Many other alternative approaches were proposed, e.g., linear seesaw [19–21], inverse seesaw [22–30], where the new physics scale responsible for neutrino mass generation can be brought down to TeV scale, at the expense of the inclusion of new additional fermion fields (S_i), which are SM singlets. Another interesting idea that has received a lot of attention in recent times is the application of modular symmetry [31–34], where the usage of excess flavon fields can naturally be avoided. In this case, the Yukawa couplings, which are holomorphic functions of modulus τ , perform the role of flavons. Here τ is a complex variable that appears in the Dedekind eta function $\eta(\tau)$ [35]. When this modulus acquires the vacuum expectation value (VEV), it breaks the flavor symmetry. There exist plentiful works in the literature based on modular groups S_3 [36, 37], S_4 [38–41], A_4 [42–62], A_5 [63, 64], double covering of A_4 [65–68], S_4 [69, 70] and A_5 [71–73]. These modular groups are quite successful in accommodating the observed neutrino oscillation parameters.

Due to the predictive features of modular symmetry group-based models, they can be probed in the forthcoming neutrino oscillation experiments. In this paper, we consider three such models and study their viability in the upcoming neutrino experiments T2HK [74],

DUNE [75] and JUNO [76]. The experiments T2HK and DUNE are the future accelerator-based long-baseline experiments, whereas JUNO is the medium baseline reactor experiment which is expected to start taking data in early 2024. The experiments T2HK and DUNE are expected to precisely measure the leptonic CP phase δ_{CP} as well as the octant of the atmospheric mixing angle θ_{23} . The experiment JUNO will further improve the measurement of θ_{12} . It is also expected that DUNE and JUNO experiments will determine the true nature of neutrino mass ordering. Also, T2HK will determine mass ordering at good significance by combining beam and atmospheric data. Currently, two orderings of the neutrino masses are allowed based on the sign of the atmospheric mass squared difference Δm_{31}^2 . The positive sign of Δm_{31}^2 gives rise to normal mass ordering, whereas the negative sign of the Δm_{31}^2 gives rise to inverted mass ordering. The rest of the parameters i.e., θ_{13} and Δm_{21}^2 are currently very well measured [77]. Here it should be mentioned that the current measurements of θ_{23} and δ_{CP} are very weak. Due to this, a large number of models are currently allowed, which predict a wide range of values regarding these two parameters. However, with the future measurements of these parameters by T2HK and DUNE, we expect to rule out many such models. One way to test these models in the neutrino experiments is to use the sum rules which connects the model parameters to the leptonic mixing parameters [78–82]. However, for the models that we consider in our study, it is not possible to derive the sum rules. In this case we numerically calculate the predicted values of the leptonic mixing parameters from these models and use them as an input while studying these models in the neutrino experiments. To the best of our knowledge this is the first work of this kind. In our work, we choose three different models in such a way that their prediction of θ_{23} and δ_{CP} are very different from each other, but still, they are allowed because of the current wide allowed ranges of these two parameters. Therefore, the main motivation of our work is to see how well future neutrino experiments will be able to constrain these models. Among these three models, we find that one of the models predicts a very narrow range of θ_{12} . This provides us an opportunity to constrain this model using JUNO. In addition, we also notice that two of the models have partially common allowed parameter space in terms of values of θ_{23} and δ_{CP} . In our work, we study the capability of DUNE and T2HK to separate these two models.

The structure of this paper is as follows. In Sec. II, we provide an overview of the theoretical framework for the three models borrowed from the original work as cited in respective subsections IIA, IIB and IIC. Further, in sec. III, we demonstrate the allowed parameter space in terms of all six neutrino oscillation parameters for these three models illustrated in IIIA, IIIB and IIIC respectively. In Sec. IV, we highlight the features and characteristics of T2HK and DUNE, which we use in our analysis. In Sec. V, we present our results, and finally, in Sec. VI, we pen down our ascertainment in conclusion.

II. MODEL FRAMEWORK

In this section, we present an overview of the models employed in our analysis, which are based on modular symmetry. Specifically, we focus on the utilization of A_4 modular symmetry to preserve the invariance of the superpotential. Our models incorporate different seesaw mechanisms to account for the tiny masses of neutrinos. Here, we provide a description of these seesaw models, including the particle content, charges, and modular weights under A_4 modular symmetry.

A. Linear Seesaw mechanism with A_4 Modular symmetry

The model considered here, which we referred to as Model-A, involves the extension of the Standard Model with an additional discrete A_4 modular symmetry. Broadly, it can be considered a modified version of a type-I seesaw that follows the flavor structure of a linear seesaw. To enrich the particle spectrum, six extra singlet heavy superfields (N_{R_i} & S_{L_i}) along with a weighton field (ρ_a) are introduced. The extra super-multiplets N_{R_i} and S_{L_i} transform as triplets under the A_4 modular group, while ρ_a transforms as a singlet. However, the modular Yukawa couplings are also charged under A_4 symmetry being a triplet with modular weight $k_I = 2$. The modular symmetry restricts the use of excessive flavon fields, which would otherwise overpopulate the particle spectrum and reduce the model's predictability when working in BSM. This is achievable because the Yukawa couplings acquire a modular form and take on the role of extra flavon fields and is applicable to subsequent models discussed in this work. The particle spectrum clubbed with modular Yukawa couplings of the model and their group charges under various symmetries, along with their modular weights, are depicted in Table I. Generally, the linear seesaw framework can be realized by assigning suitable charges under different groups to the comprising particles.

Additionally, the model has an additional $U(1)_X$ global symmetry as outlined in the original paper [83], enforced to eliminate certain undesirable terms in the superpotential. The A_4 symmetry is believed to be broken at a scale much higher than the electroweak symmetry breaking [84]. The masses of the additional superfields are generated by assigning a non-zero vacuum expectation value to the singlet weighton.

The invariant super-potential in the present model framework is represented as:

$$\begin{aligned} \mathcal{W} = & y_\ell^{\wp\wp} L_{\wp L} H_d \wp_R^c + G_D L_{\wp L} H_u (\mathbf{Y} N_R)_{1,1'',1'} + G'_D [L_{\wp L} H_u (\mathbf{Y} S_L^c)_{1,1',1''}] \frac{\rho_a^3}{\Lambda_a^3} \\ & + [\alpha_{NS} \mathbf{Y} (S_L^c N_R)_{\text{sym}} + \beta_{NS} \mathbf{Y} (S_L^c N_R)_{\text{Anti-sym}}] \rho_a , \end{aligned} \quad (1)$$

where, $G_D = \text{diag}(\alpha_D, \beta_D, \gamma_D)$ and $G'_D = \text{diag}(\alpha'_D, \beta'_D, \gamma'_D)$ being the diagonal matrices containing six free parameters, α_{NS} and β_{NS} are other free parameters involved in the superpotential and $\wp = (e, \mu, \tau)$ corresponding to the lepton flavors and Λ_a is the cut-off scale.

	Fermions						Scalars		Yukawa couplings
Fields	e_R^c	μ_R^c	τ_R^c	$L_{\phi L}$	N_R	S_L^c	$H_{u,d}$	ρ_a	$\mathbf{Y} = (y_1, y_2, y_3)$
$SU(2)_L$	1	1	1	2	1	1	2	1	—
$U(1)_Y$	1	1	1	$-\frac{1}{2}$	0	0	$\frac{1}{2}, -\frac{1}{2}$	0	—
$U(1)_X$	1	1	1	-1	1	-2	0	1	—
A_4	1	1'	1''	$1, 1'', 1'$	3	3	1	1	3
k_I	1	1	1	-1	-1	-1	0	0	2

TABLE I: Particle content and modular Yukawa couplings of the model and their charges under $SU(2)_L \times U(1)_Y \times U(1)_X \times A_4$ where k_I is the number of modular weight.

Depending upon the charge assignment to left-handed (LH) and right-handed (RH) charged leptons, which are singlets under A_4 , the charged lepton mass matrix obtained from the first term in Eq.(1), is found to be diagonal, and the couplings can be adjusted to achieve the observed charged lepton masses. The mass matrix takes the form

$$M_\ell = \begin{pmatrix} y_\ell^{ee} v_d / \sqrt{2} & 0 & 0 \\ 0 & y_\ell^{\mu\mu} v_d / \sqrt{2} & 0 \\ 0 & 0 & y_\ell^{\tau\tau} v_d / \sqrt{2} \end{pmatrix} = \begin{pmatrix} m_e & 0 & 0 \\ 0 & m_\mu & 0 \\ 0 & 0 & m_\tau \end{pmatrix}. \quad (2)$$

Here, m_e , m_μ , and m_τ are the observed charged lepton masses. Further, in Eq.(1) the second term involves N_{R_i} , which being an A_4 triplet, its contraction happens with triplet modular Yukawa coupling Y , hence resulting the Dirac neutrino mass matrix shown below

$$M_D = \frac{v_u}{\sqrt{2}} \begin{bmatrix} \alpha_D & 0 & 0 \\ 0 & \beta_D & 0 \\ 0 & 0 & \gamma_D \end{bmatrix} \begin{bmatrix} y_1 & y_3 & y_2 \\ y_2 & y_1 & y_3 \\ y_3 & y_2 & y_1 \end{bmatrix}_{LR}. \quad (3)$$

Similarly, the flavor structure for the pseudo-Dirac term is due to the contraction of A_4 triplet S_{L_i} with modular Yukawa coupling Y , and its mass matrix takes the form,

$$M_{LS} = \frac{v_u}{\sqrt{2}} \left(\frac{v_{\rho_a}}{\sqrt{2}\Lambda_a} \right)^3 \begin{bmatrix} \alpha'_D & 0 & 0 \\ 0 & \beta'_D & 0 \\ 0 & 0 & \gamma'_D \end{bmatrix} \begin{bmatrix} y_1 & y_3 & y_2 \\ y_2 & y_1 & y_3 \\ y_3 & y_2 & y_1 \end{bmatrix}_{LR}, \quad (4)$$

where, v_u , v_d and v_{ρ_a} are the VEV of H_u , H_d and ρ_a respectively. Finally, the mixing between the heavy fermions N_{R_i} and S_{L_i} results in a mass matrix consisting of both symmetric and anti-symmetric matrices with $\alpha_{NS} \gg \beta_{NS}$ as given below,

$$M_{RS} = \frac{v_{\rho_a}}{\sqrt{2}} \left(\frac{\alpha_{NS}}{3} \begin{bmatrix} 2y_1 & -y_3 & -y_2 \\ -y_3 & 2y_2 & -y_1 \\ -y_2 & -y_1 & 2y_3 \end{bmatrix}_{sym} + \beta_{NS} \begin{bmatrix} 0 & y_3 & -y_2 \\ -y_3 & 0 & y_1 \\ y_2 & -y_1 & 0 \end{bmatrix}_{asym} \right). \quad (5)$$

The linear seesaw is a modified form of type-I seesaw, and the mass formula for light neutrinos in this framework is given by

$$m_\nu = -M_D M_{RS}^{-1} M_{LS}^T + \text{transpose} . \quad (6)$$

B. Type-I seesaw without any flavon fields

Here, we consider another model based on the A_4 modular symmetry proposed by Feruglio [33] identified as Model-B. In this model, the Higgs¹ and lepton super-fields undergo specific transformations, which are detailed in Table II. This model is free from extra flavon fields and only includes three right-handed (RH) neutrinos.

	Fermions					Scalars	Yukawa couplings
Fields	E_{1R}^c	E_{2R}^c	E_{3R}^c	L	N_R^c	$H_{u,d}$	$\mathbf{Y} = (y_1, y_2, y_3)$
$SU(2)_L$	1	1	1	2	1	2	—
$U(1)_Y$	1	1	1	$-\frac{1}{2}$	0	$\frac{1}{2}, -\frac{1}{2}$	—
A_4	1	$1''$	$1'$	3	3	1	3
k_I	1	1	1	1	1	0	2

TABLE II: Particle content and Yukawa couplings under $SU(2)_L \times U(1)_Y \times A_4$ modular symmetry, where, k_I being the modular weight.

The super-potential of the model can be expressed as

$$\mathcal{W} = w_e + w_\nu , \quad (7)$$

with $w_e = \alpha_l E_1^c H_d (LY)_1 + \beta_l E_2^c H_d (LY)_{1'} + \gamma_l E_3^c H_d (LY)_{1''} , \quad (8)$

and $w_\nu = g(N_R^c H_u LY)_1 + \Lambda_b (N_R^c N_R^c Y)_1 , \quad (9)$

where, $g, \alpha_l, \beta_l, \gamma_l$ are the free parameters and Λ_b is the cut-off mass parameter. The mass matrix for the charged lepton sector is a non-diagonal matrix because the left and right-handed charged leptons are triplets and singlets, and, due to the product rule of A_4 symmetry, they attain a form given below.

$$M_L = \frac{v_d}{\sqrt{2}} \begin{pmatrix} \alpha_l y_1 & \alpha_l y_3 & \alpha_l y_2 \\ \beta_l y_2 & \beta_l y_1 & \beta_l y_3 \\ \gamma_l y_3 & \gamma_l y_2 & \gamma_l y_1 \end{pmatrix} , \quad (10)$$

¹ The super-multiplet's (i.e., H_u & H_d) VEV are related to SM Higgs VEV by the relation $v_H = \frac{1}{2}\sqrt{v_u^2 + v_d^2}$, and $\tan \beta = (v_u/v_d)$.

where v_d is the VEV of H_d , and the free parameters can be determined by using the below identities:

$$\begin{aligned}\text{Det}(M_L M_L^\dagger) &= m_e^2 m_\mu^2 m_\tau^2, \\ \text{Tr}(M_L M_L^\dagger) &= m_e^2 + m_\mu^2 + m_\tau^2, \\ \frac{1}{2} \left([\text{Tr}(M_L M_L^\dagger)]^2 - [\text{Tr}(M_L M_L^\dagger)^2] \right) &= m_e^2 m_\mu^2 + m_\mu^2 m_\tau^2 + m_\tau^2 m_e^2,\end{aligned}\quad (11)$$

where, m_e , m_μ and m_τ are the charged lepton masses [85]. Further, the Dirac mass matrix emerges as given below due to contraction between LH lepton doublets, RH neutrinos, and modular Yukawa couplings as they are A_4 triplets.

$$M_D = \frac{v_u}{\sqrt{2}} \begin{pmatrix} 2\mathbf{g}_1 y_1 & (-\mathbf{g}_1 + \mathbf{g}_2) y_3 & (-\mathbf{g}_1 - \mathbf{g}_2) y_2 \\ (-\mathbf{g}_1 - \mathbf{g}_2) y_3 & 2\mathbf{g}_1 y_2 & (-\mathbf{g}_1 + \mathbf{g}_2) y_1 \\ (-\mathbf{g}_1 + \mathbf{g}_2) y_2 & (-\mathbf{g}_1 - \mathbf{g}_2) y_1 & 2\mathbf{g}_1 y_3 \end{pmatrix}. \quad (12)$$

where, v_u is the VEV of H_u . Finally, the Majorana mass matrix for heavy right-handed neutrinos obtained from the second term of eqn.(9), expressed as

$$M_R = \begin{pmatrix} 2y_1 & -y_3 & -y_2 \\ -y_3 & 2y_2 & -y_1 \\ -y_2 & -y_1 & 2y_3 \end{pmatrix} \Lambda_b. \quad (13)$$

As it is a type-I seesaw mechanism hence, the light neutrino mass formula is given by

$$m_\nu = -M_D M_R^{-1} M_D^T. \quad (14)$$

C. Type-III seesaw

	Fermions					Scalars		Yukawa couplings
Fields	E_{1R}^c	E_{2R}^c	E_{3R}^c	L	$\Sigma_{R_i}^c$	$H_{u,d}$	ρ_c	$\mathbf{Y} = (y_1, y_2, y_3)$
$SU(2)_L$	1	1	1	2	3	2	1	—
$U(1)_Y$	1	1	1	$-\frac{1}{2}$	0	$\frac{1}{2}, -\frac{1}{2}$	0	—
$U(1)_{B-L}$	1	1	1	-1	1	0	-2	—
A_4	1	1'	1''	1, 1'', 1'	3	1	1	3
k_I	0	0	0	0	-2	0	2	2

TABLE III: Particle content and Yukawa couplings of the type-III seesaw and their charges under $SU(2)_L \times U(1)_Y \times U(1)_{B-L} \times A_4$, and k_I is the modular weight.

The model considered here, referred to as Model-C, employs a type-III seesaw mechanism with A_4 modular symmetry and $U(1)_{B-L}$ symmetry in addition to SM symmetries. The

model comprises BSM particles, i.e., three right-handed fermion triplets (Σ_{R_i}) and weighton (ρ_c). Hence, A_4 symmetry and $U(1)_{B-L}$ symmetries are broken at a significantly high scale than the electroweak symmetry-breaking scale. Table (III) provides the A_4 charges and modular weights for the added particles with elaborated discussion present in original work [86]. The purpose of incorporating extra $U(1)_{B-L}$ symmetry is to avoid undesirable terms in the superpotential, which cannot be prevented by A_4 modular symmetry alone. The non-zero VEV of the singlet weighton aids in providing mass to the heavy RH neutrinos. The complete superpotential of the model is given as

$$\begin{aligned} \mathcal{W} = & -y_{ij}E_{R_i}^c H_d L_j - (\alpha_\Sigma)_{ij} \left[H_u \Sigma_{R_i}^c \sqrt{2} \mathbf{Y} L_j \right] \\ & - \frac{M'_\Sigma}{2} \left(\beta_\Sigma \text{Tr} [\Sigma_{\mathbf{R}_i}^c \mathbf{Y} \Sigma_{\mathbf{R}_i}^c]_s + \gamma'_\Sigma \text{Tr} [\Sigma_{\mathbf{R}_i}^c \mathbf{Y} \Sigma_{\mathbf{R}_i}^c]_a \right) \frac{\rho_c}{\Lambda_c}, \end{aligned} \quad (15)$$

where, $\alpha_\Sigma = \text{diag}(a_1, a_2, a_3)$, $\beta_\Sigma = \text{diag}(b_1, b_2, b_3)$ and $\gamma'_\Sigma = \text{diag}(\gamma_1, \gamma_2, \gamma_3)$ representing free parameter diagonal matrices, with M'_Σ as the free mass parameter and Λ_c is the cut-off scale with the charged lepton mass matrix being diagonal, similar to, as depicted in Model-A. The interaction between the neutral multiplet of a fermion triplet and the LH neutrino leads to the Dirac mass term, which determines the Dirac mass matrix:

$$M_D = v_u \begin{bmatrix} a_1 & 0 & 0 \\ 0 & a_2 & 0 \\ 0 & 0 & a_3 \end{bmatrix} \begin{bmatrix} y_1 & y_3 & y_2 \\ y_2 & y_1 & y_3 \\ y_3 & y_2 & y_1 \end{bmatrix}, \quad (16)$$

where, v_u is the VEV of H_u and the Majorana mass matrix is given as,

$$M_R = \frac{v_{\rho_c}}{\Lambda_c \sqrt{2}} \left(\frac{M'_\Sigma}{2} \right) \left(\frac{\beta_\Sigma}{3} \begin{bmatrix} 2y_1 & -y_3 & -y_2 \\ -y_3 & 2y_2 & -y_1 \\ -y_2 & -y_1 & 2y_3 \end{bmatrix}_{sym} + \gamma'_\Sigma \begin{bmatrix} 0 & y_3 & -y_2 \\ -y_3 & 0 & y_1 \\ y_2 & -y_1 & 0 \end{bmatrix}_{asym} \right), \quad (17)$$

where, v_{ρ_c} is the VEV of ρ_c . The mass matrix for active neutrinos within the type-III seesaw framework is expressed as follows:

$$m_\nu = -M_D M_R^{-1} M_D^T. \quad (18)$$

III. PREDICTION OF THE LEPTONIC MIXING PARAMETERS FROM THE MODELS

This section is accentuated for discussing the results obtained for three different models whose theoretical frameworks are aforementioned in Sec. II. In order to conduct numerical

Osc. Parameters	$\sin^2 \theta_{12}$	$\sin^2 \theta_{23}$	$\sin^2 \theta_{13}$	Δm_{21}^2 [eV ²]	$ \Delta m_{31}^2 $ [eV ²]	δ_{CP}
Nu-Fit (NH)	0.303	0.451	0.02225	7.41×10^{-5}	2.507×10^{-3}	232°
Nu-Fit (IH)	0.303	0.569	0.02223	7.41×10^{-5}	2.486×10^{-3}	276°
Model-A	0.315	0.428	0.02343	7.65×10^{-5}	2.502×10^{-3}	45.30°
Model-B	0.340	0.452	0.02138	7.73×10^{-5}	2.474×10^{-3}	0°
Model-C	0.308	0.469	0.02169	7.17×10^{-5}	2.461×10^{-3}	213.18°

TABLE IV: In the above table, we elucidate the best-fit value for the oscillation parameters (i.e., mixing angles $\sin^2 \theta_{12}$, $\sin^2 \theta_{23}$ & $\sin^2 \theta_{13}$ and mass squared differences (Δm_{21}^2 and Δm_{31}^2) and δ_{CP} phase.)

analysis, we are utilizing the NuFIT neutrino oscillation data from [77, 87] at a 3σ interval as follows:

$$\begin{aligned} \text{NO : } \sin^2 \theta_{13} &= [0.02052, 0.02398], \quad \sin^2 \theta_{23} = [0.408, 0.603], \quad \sin^2 \theta_{12} = [0.270, 0.341], \\ \Delta m_{31}^2 &= [2.427, 2.59] \times 10^{-3} \text{ eV}^2, \quad \Delta m_{21}^2 = [6.82, 8.03] \times 10^{-5} \text{ eV}^2, \end{aligned} \quad (19)$$

$$\begin{aligned} \text{IO : } \sin^2 \theta_{13} &= [0.02048, 0.02416], \quad \sin^2 \theta_{23} = [0.412, 0.613], \quad \sin^2 \theta_{12} = [0.270, 0.341], \\ |\Delta m_{31}^2| &= [2.406, 2.57] \times 10^{-3} \text{ eV}^2, \quad \Delta m_{21}^2 = [6.82, 8.03] \times 10^{-5} \text{ eV}^2. \end{aligned} \quad (20)$$

Here, we numerically diagonalize the neutrino mass matrices for each model through the relation $U^\dagger \mathcal{M} U = \text{diag}(m_1^2, m_2^2, m_3^2)$, where $\mathcal{M} = m_\nu m_\nu^\dagger$ and U is a unitary matrix² from which the neutrino mixing angles can be extracted using the standard relations:

$$\sin^2 \theta_{13} = |U_{13}|^2, \quad \sin^2 \theta_{23} = \frac{|U_{23}|^2}{1 - |U_{13}|^2}, \quad \sin^2 \theta_{12} = \frac{|U_{12}|^2}{1 - |U_{13}|^2}. \quad (21)$$

The input parameters are randomly scanned over for each model individually, and presented in Tables V, VI and VII for Model-A, Model-B, and Model-C, respectively. The parameter space for the allowed regions is initially filtered by the observed 3σ limit of solar and atmospheric mass squared differences and further constrained by mixing angles and the observed sum of active neutrino masses $0.058 \leq \Sigma m_{\nu_i} \leq 0.12$ eV [89, 90] ($i=1,2,3$), for Model-A and Model-C as these models satisfy normal hierarchy and $0.098 \leq \Sigma m_{\nu_i} \leq 0.12$ eV [91] for Model-B, which follows the inverted hierarchy. The best-fit values of the input parameters are obtained by utilizing the chi-square minimization technique and the general chi-square formula [92, 93],

$$\chi^2 = \sum_i \left(\frac{T_i(z) - E_i}{\sigma_i} \right)^2, \quad (22)$$

² For non-diagonal charged lepton sector the lepton mixing matrix is given as $U' = U_l^\dagger U$, where, U_l matrix diagonalizes the charged lepton mass matrix [88].

where E_i is the experimentally observed best-fit value of oscillation parameters from NuFIT and $T_i(z)$ is the theoretical prediction for the corresponding oscillation parameter as a function of z , where z indicates input parameters in the model, while σ_i is the 1σ errors in E_i .

By examining the values of the input parameters within their respective ranges, we calculate the χ^2 for all available observables in the neutrino sector, which include two mass-squared differences, three mixing angles, and CP phase (δ_{CP}). These calculations yield a cumulative χ^2 minimum, which we use to determine the values of the free parameters that correspond to the minimum, also known as the best-fit values. By employing these best-fit values of the input parameters, we can refine the ranges for each model parameter by aligning them closely around these values. By adopting this approach, we can generate model predictions by placing emphasis on the parameter value that is most likely. Next, we highlight the nitty-gritty of the model parameter space for each case below.

A. Model-A

To fit the current neutrino oscillation data, we chose the ranges for the model parameters as shown in Table V,

Parameter	Range	Parameter	range
$\text{Re}[\tau]$	$[-0.5, 0.5]$	β'_D	$[6.0 - 9.9] \times 10^{-3}$
$\text{Im}[\tau]$	$[1.2, 1.8]$	γ'_D	$[3.2 - 8.3] \times 10^{-3}$
α_D	$[6.7 - 9.7] \times 10^{-6}$	α_{NS}	$[0.1 - 0.24]$
β_D	$[4.4 - 4.8] \times 10^{-6}$	β_{NS}	$[1 - 2.2] \times 10^{-5}$
γ_D	$[5.2 - 8.8] \times 10^{-6}$	Λ_a	$[10^5, 10^6] \text{ GeV}$
α'_D	$[2.3 - 6.3] \times 10^{-3}$	v_{ρ_a}	$[10^4, 10^5] \text{ GeV}$

TABLE V: Model parameters ranges for Model-A

The prediction of the leptonic mixing parameters for Model-A is shown in the top row of Fig. 1. From the panels, we see that the model allows all the values of the parameters θ_{12} , θ_{13} , θ_{23} , Δm_{21}^2 and Δm_{31}^2 within the current 3σ values of their global fit except δ_{CP} . The allowed values of δ_{CP} lies within the range of $0^\circ \leq \delta_{\text{CP}} < 89^\circ$. As the T2HK and DUNE will be able to measure δ_{CP} very precisely, this model can be constrained in the future based on the data from these two experiments. The best-fit values of the oscillation parameters as obtained from this model are listed in the third row of Table IV.

B. Model-B

Similarly, we showcase the model parameter space in Table VI, which satisfies the neutrino experimental data. The prediction of this model in terms of the neutrino oscillation

$\text{Re}(\tau)$	$\text{Im}(\tau)$	g_1	g_2	Λ_b [GeV]
$[-0.1, 0.1]$	$[1.5, 2.0]$	$[1, 3] \times 10^{-5}$	$[2, 5] \times 10^{-5}$	$[10^6, 10^7]$

TABLE VI: Ranges required for input parameters in Model-B

parameters is shown in the middle row of Fig. 1. For this model, the parameters θ_{13} and Δm_{21}^2 are unconstrained. For Δm_{31}^2 this model disallows a small region around the lower edge of the 3σ bound for this parameter, i.e., $|\Delta m_{31}^2| < 2.43 \times 10^{-3}$. This model allows only $\delta_{\text{CP}} = 0^\circ$. Additionally, this model predicts lower octant of θ_{23} , i.e., $\sin^2 \theta_{23} < 0.459$ and also a narrow range of θ_{12} with $\sin^2 \theta_{12}$ around 0.34 which lies in the upper edge of the current 3σ according to NuFIT. Therefore, this model can be constrained by all three experiments that we consider in this present study. The prediction of θ_{23} and δ_{CP} can be constrained by DUNE and T2HK, whereas the prediction of θ_{12} can be constrained by JUNO. Note that the allowed region of Model-B is basically a part of the allowed parameter space of Model-A in terms of parameter θ_{23} and δ_{CP} . Therefore it will be interesting to see the capability of DUNE and T2HK to distinguish these two models. The best-fit values of the oscillation parameters as obtained from this model are listed in the fourth row of Table IV.

Here it should be mentioned that Model-A is allowed for normal ordering of the neutrino masses, whereas Model-B is allowed for the inverted ordering. Therefore, once the true mass ordering of the neutrinos is determined, one of these models will be excluded immediately. However, in this study, we assume that both the mass ordering of the neutrinos are allowed, and we will study the distinguishability of these two models in DUNE and T2HK based on their prediction of the leptonic mixing parameters.

C. Model-C

Finally, the parameter space for Model-C, satisfying the ranges of the neutrino experimental bounds, is depicted in Table VII.

The parameter prediction of Model-C is shown in the bottom row of Fig. 1. From the panels, we see that all the parameters except δ_{CP} are unconstrained in this model. However, there exists a correlation between θ_{13} and Δm_{31}^2 as certain combinations of these parameters are not allowed. The allowed values of δ_{CP} for this model lies in the range of $162^\circ < \delta_{\text{CP}} < 256^\circ$. As the δ_{CP} values allowed from this model are very disjoint from the other two models, this model can be easily differentiated from them. The best-fit values of the oscillation parameters as obtained from this model are listed in the fifth column of Table IV.

Parameter	Range	Parameter	range
$\text{Re}[\tau]$	$[-0.5, 0.5]$	b_2	$[0.8 - 8] \times 10^{-1}$
$\text{Im}[\tau]$	$[0.75, 2]$	b_3	$[1 - 7] \times 10^{-3}$
a_1	$[5 - 10] \times 10^{-7}$	γ_Σ	$[0.1, 1] \times 10^{-9}$
a_2	$[4.5 - 10] \times 10^{-6}$	M'_Σ	$[10^7, 10^8] \text{ GeV}$
a_3	$[0.5 - 5] \times 10^{-7}$	Λ_c	$[10^7, 10^8] \text{ GeV}$
b_1	$[0.7 - 5] \times 10^{-2}$	v_{ρ_c}	$[10^6, 10^7] \text{ GeV}$

TABLE VII: Ranges required for free parameters in Model-C

IV. EXPERIMENTAL CHARACTERISTICS

To simulate the experiments T2HK, DUNE and JUNO, we use the software GLoBES [94, 95]. Below we describe the specification of these experiments that we use in our calculation.

DUNE (Deep Underground Neutrino Experiment) is a future accelerator-based long-baseline experiment that features a 1284.9 km baseline with the line-averaged Earth-matter constant density 2.84 g/cm^3 and a 40 kton liquid Argon time projection chamber as far detector. The neutrino source for this experiment can provide 1.1×10^{21} protons on target (POT) per year with a beam power of 1.2 MW. In this case, the flux will be an on-axis wide-band flux. Our estimation of the physics capabilities of this set-up is based on assuming 5 years of neutrino run and 5 years of anti-neutrino run. The specifications regarding backgrounds, systematic errors, etc., are taken from [96].

T2HK (Tokai-to-Hyper-Kamiokande) is another upcoming long baseline experiment with baseline length of 295 km and is off-axial by 2.5° , producing a very narrow beam. For T2HK, we have used the configuration provided in Ref. [74]. The neutrino source, stationed at J-PARC, will operate at a beam power of 1.3 MW and will have a total exposure of 27×10^{21} protons on target (POT), equivalent to ten years of operation. The 10 years of runtime has been divided into two equal periods of five years each, one for neutrino and the other for antineutrino mode. The averaged Earth matter density for this baseline is around 2.70 g/cm^3 , and the detector technology will be water Cherenkov having a fiducial volume of 374 kt.

For JUNO, we follow the configuration as given in Ref. [76]. We consider a liquid scintillator detector having 20 kton fiducial mass located at a distance of around 53 km from Yangjiang and Taishan nuclear power plants. We have considered the energy resolution of $3\%/\sqrt{E} \text{ (MeV)}$. In this analysis, we consider all the reactor cores located at the same

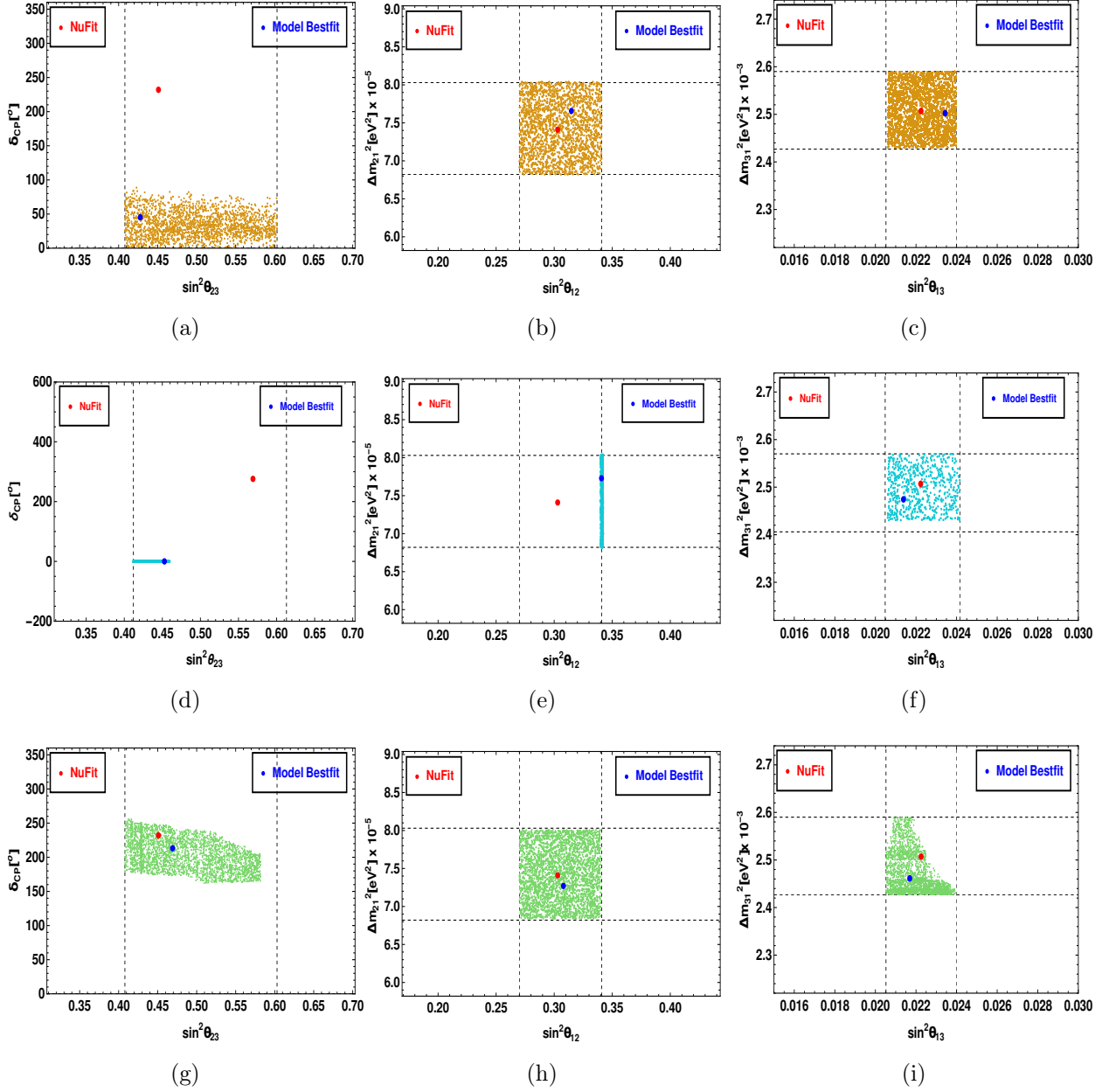


FIG. 1: The panels 1a, 1d and 1g illustrate the correlation of $\sin^2 \theta_{23}$ w.r.t δ_{CP} phase for Model-A, B and C, respectively and 1b, 1e and 1h (1c, 1f and 1i) project the inter-dependence of Δm_{21}^2 (Δm_{31}^2) w.r.t to $\sin^2 \theta_{12}$ ($\sin^2 \theta_{13}$) for Model-A, B and C respectively. Here the vertical and horizontal gridlines show the 3σ range of the corresponding oscillation parameters. Also, the NuFIT and model best-fit is shown by a red and blue dot, respectively.

distance from the detector. We consider the run-time to be 6 years.

V. RESULTS

In this section, we will present our results. First, we study the capability of T2HK, DUNE, and JUNO to constrain the three models that we discussed above with respect to the current data. Then we study the capability of these experiments to differentiate one model from another.

We will present our results in terms of χ^2 analysis. We define the Poisson χ^2 as:

$$\chi^2 = 2 \sum_j \left[N_j^{\text{th}} - N_j^{\text{true}} - N_j^{\text{true}} \ln \left(\frac{N_j^{\text{th}}}{N_j^{\text{true}}} \right) \right], \quad (23)$$

where j is the number of energy bins, N_j^{th} is the number of events in the test spectrum and N_j^{true} is the number of events in the true spectrum.

To test the models against the current values of oscillation parameters, we take the current values of the oscillation parameters in the true and the values of the oscillation parameters predicted from the models in the test. For each set of true parameters, we minimize the χ^2 with respect to all sets of predicted parameters. We find the minimum χ^2 i.e., χ_{\min}^2 for all sets of true parameters and calculate $\Delta\chi^2$ as $\chi^2 - \chi_{\min}^2$. As, Model-A and Model-C are allowed for the normal ordering of the neutrino masses, for these models, we use the true values from NuFIT corresponding to normal ordering in the neutrino masses. However, for Model-B, we use the NuFIT values corresponding to the inverted ordering of the neutrino masses. The best-fit values from NuFIT for both normal and inverted ordering of the neutrino masses are listed in the first and second row of Table IV.

These results are presented in Fig. 2. The first row is for Model-A, the second row is for Model-B, and the third row is for Model-C. For all three models, we have presented the sensitivity in the θ_{23} (true) - δ_{CP} (true) plane for DUNE and T2HK. In those panels, we have shown the allowed regions corresponding to 3σ (blue curve) and 5σ C.L (brown curve). The best-fit values of θ_{23} and δ_{CP} for these allowed regions are indicated by a red asterisk. Additionally, in these panels, the current 1σ and 2σ allowed regions from NuFIT are shown in the orange and purple-shaded regions, respectively. The best-fit values from the NuFIT is shown by the black asterisk. Assuming the current best-fit values of θ_{23} and δ_{CP} remain the same in future, DUNE and T2HK will measure these values very precisely. The yellow shaded and the cyan shaded region show the allowed region from DUNE and T2HK at 3σ C.L, respectively, with respect to the current best-fit value of θ_{23} and δ_{CP} . Therefore, the yellow and cyan regions show how much the orange and the purple region will shrink in the future by the measurements of DUNE and T2HK. In the next paragraph, we will discuss the capability of T2HK and DUNE to exclude these models, assuming the current best-fit

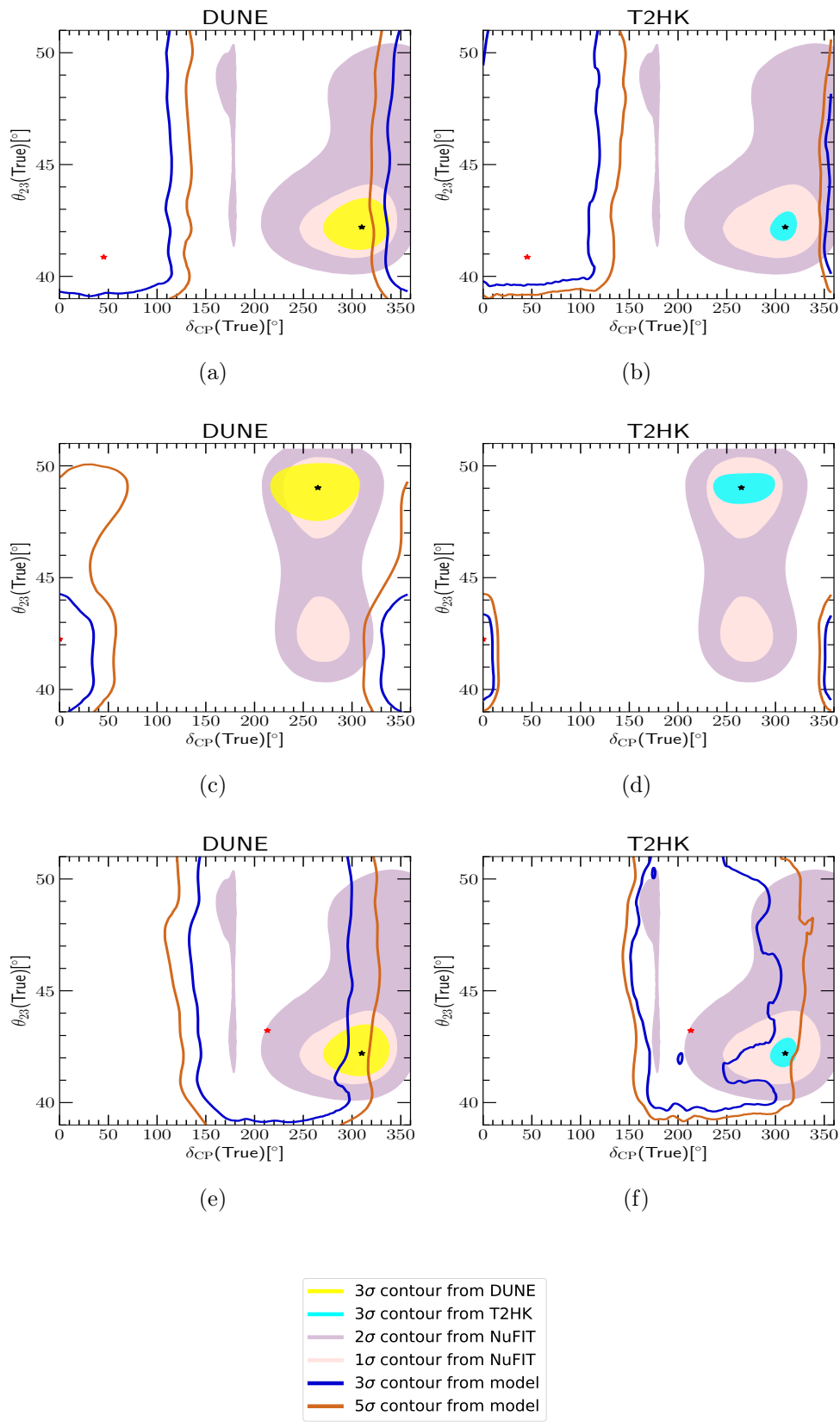


FIG. 2: Panels representing the sensitivity of DUNE and T2HK in θ_{23} (true) - δ_{CP} (true) plane. Panel 2a, 2c and 2e represent the compatibility of Model-A, B, and C with DUNE, respectively, while panel 2b, 2d and 2f represent the compatibility of the same models with T2HK. The black and red asterisks correspond to the NuFIT and model best-fit, respectively.

values remain the same in the future and they are measured by T2HK and DUNE. Or in other words, we will compare the allowed regions given by the blue and brown curves with respect to the yellow region for DUNE and the cyan region for T2HK.

From this figure, in general, we see that the allowed regions for all three models are more constrained in T2HK as compared to DUNE. This is probably because of the large statistics of T2HK, which arises due to its shorter baseline as compared to DUNE. For Model-A, we see that the 5σ allowed region is well separated from the 3σ allowed region for T2HK, but for DUNE, they are consistent. However, the 3σ C.L. region of Model-A will not be compatible with the 3σ allowed region of DUNE. For Model-B, the 5σ allowed region will not overlap with the 3σ allowed region of both T2HK and DUNE if the future best-fit values of θ_{23} and δ_{CP} remain same as the current best-fit value. Further, it will be difficult for both T2HK and DUNE to exclude Model-C as, in this case, the 5σ allowed region of this model remains consistent with the 3σ C.L. allowed regions of T2HK and DUNE. However, the 3σ allowed region of Model-C is incompatible with the 3σ allowed region of T2HK.

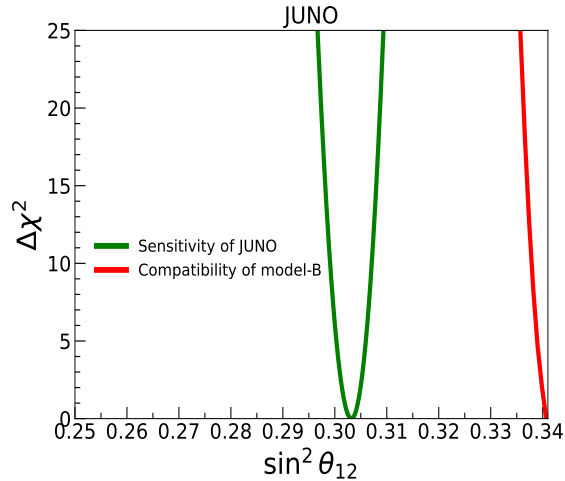


FIG. 3: Figure illustrating the sensitivity of JUNO to constrain Model-B. The green solid curve shows the future precision of θ_{12} with respect to the current best fit of this parameter. The red solid curve represents allowed values of θ_{12} by JUNO for Model-B.

In the previous section, we have seen that Model-B predicts a very narrow range of θ_{12} , and this gives us an opportunity to constrain this model from the future data of JUNO. In Fig. 3, we have shown the capability of JUNO to constrain this model (red curve). In this figure, the green curve shows the sensitivity of JUNO to constrain the parameter θ_{12} , given its best-fit remains at the current best-fit value in the future. From this figure, we observe that the future allowed values of θ_{12} by JUNO are very much separated from the allowed values of θ_{12} by Model-B. Therefore, JUNO alone will be able to exclude this model at an extremely high confidence level.

Now let us discuss the capability of DUNE and T2HK to separate one model from another. In the previous section, we have seen that Model-A and Model-B have some common allowed

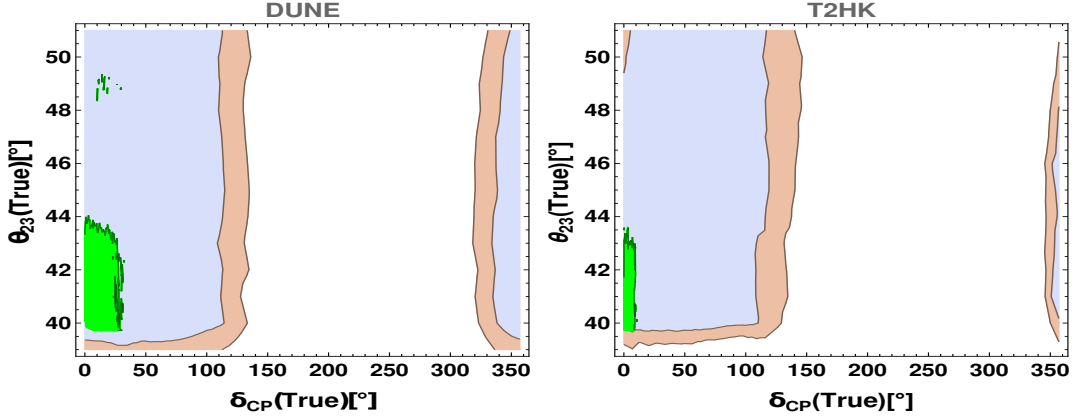


FIG. 4: The blue (brown) shaded regions in the panels represent the 3σ (5σ) allowed regions of Model-A, while the green region corresponds to the parameter space for which Model-B cannot be separated from Model-A at 3σ C.L. The left panel is for DUNE and the right panel is for T2HK.

parameter space in terms of θ_{23} and δ_{CP} . However, the allowed region of Model-C in θ_{23} - δ_{CP} parameter space is disjoint with respect to Model-A and Model-B. This implies that Model-C can be easily separated from Model-A and Model-B in DUNE and T2HK, whereas these experiments will have confusion to separate Model-A from Model-B. We have shown this in Fig. 4. The left panel is for DUNE, and the right panel is for T2HK. To generate this figure, we have taken Model-A in the true spectrum of the χ^2 and Model-B in the test spectrum. For each set of true parameters for Model-A, we have minimized over all sets of test parameters from Model-B and presented the results in the δ_{CP} (true) - θ_{23} (true) plane for Model-A. Here also, we have subtracted the overall χ^2_{min} from each χ^2 to calculate the $\Delta\chi^2$. This $\Delta\chi^2$ is represented in these panels as green allowed regions at 3σ C.L. In these panels, blue and brown regions are the allowed region for Model-A at 3σ C.L and 5σ C.L., respectively. Therefore, we understand that in the green region, DUNE, and T2HK will not be capable of separating Model-A from Model-B. However, in the rest of the blue and brown regions, DUNE and T2HK will be able to distinguish between Model-A and Model-B. Here also, we see that the confusion between Model-A and Model-B will be more prominent in DUNE as compared to T2HK.

VI. CONCLUSION

This paper explores the potential of upcoming neutrino experiments to constrain a series of theoretical models that utilize modular symmetry. Here, we make use of A_4 modular symmetry, which is favorable in eliminating the excess usage of flavon fields. In lieu of traditional flavon fields, the model incorporated modular Yukawa couplings that transformed non-trivially under a modular A_4 group, resulting in a unique flavor structure of the neu-

trino mass matrix and facilitating the study of neutrino phenomenology. The models under scrutiny are linear seesaw identified as Model-A and involves three right-handed (RH) (N_R) and three left-handed (LH) sterile (S_L) superfields and a weighton (ρ_a); Model-B is a type-I seesaw utilizing three RH (N_R) without any flavons, and Model-C is a type-III seesaw involving fermion triplets superfields (Σ_R) and a weighton (ρ_c) in supersymmetric context. These models based on modular symmetry can predict the values of the leptonic mixing parameters, and therefore, there is an opportunity to probe these models in the neutrino oscillation experiments.

We choose our models in such a way that their predictions of the neutrino oscillation parameters are different from each other, but these models are allowed within the currently allowed ranges of these parameters. Among the three models, Model-A and Model-C are allowed for the normal ordering of the neutrino masses, whereas Model-B is allowed for the inverted ordering of the neutrino masses. For our analysis, we have considered the future accelerator-based neutrino experiments T2HK and DUNE and also the medium-baseline reactor experiment JUNO. The experiments T2HK and DUNE are expected to measure the parameters θ_{23} and δ_{CP} with excellent precision, whereas JUNO will provide the most stringent measurement of θ_{12} . As the three models that we consider in our study provide narrow ranges of the oscillation parameters θ_{23} , θ_{12} and δ_{CP} , the experiments T2HK, DUNE and JUNO will have the capability to constrain these models in future. Apart from that, it is also expected that DUNE, T2HK and JUNO will discover the true nature of the neutrino mass ordering. Note that once the true mass ordering of the neutrino masses is determined, either Model-A and Model-C or Model-B can be excluded immediately. However, in this work, we will assume that neutrino mass ordering will be unknown, and we will study these models in future neutrino experiments based on their prediction of the neutrino oscillation parameters. For our models, it is not possible to define the sum rules which relate the model parameters to the leptonic mixing parameters. Therefore we adopted the strategy to estimate the prediction of the models numerically and then used them as input for studying these models in the neutrino experiments.

Among the three models that we consider in our study, Model-A predicts the values of δ_{CP} to lie in the range of $0^\circ \leq \delta_{\text{CP}} < 89^\circ$. Model-B allows only $\delta_{\text{CP}} = 0^\circ$ and predicts lower octant of θ_{23} in the region $\sin^2 \theta_{23} < 0.459$. It also predicts a narrow range of θ_{12} with $\sin^2 \theta_{12}$ around 0.34. The allowed values of δ_{CP} for Model-C lie in the range of $162^\circ < \delta_{\text{CP}} < 256^\circ$. When studying these models in the neutrino experiments, we find that capability of T2HK to constrain the models is better as compared to DUNE. Assuming the future best-fit of θ_{23} and δ_{CP} remains the same as the current one, we noticed that T2HK could exclude Model-A at more than 5σ C.L, but this model will be consistent with DUNE at 5σ C.L. For Model-B, both T2HK, and DUNE will be capable of excluding this model at more than 5σ C.L. Model-C cannot be excluded by T2HK and DUNE at 5σ C.L. Further, our results show that JUNO alone can exclude Model-B at an extremely high confidence level if the future best-fit of θ_{12} remains at the current-one. As Model-A and Model-B have a common

parameter space in terms of θ_{23} and δ_{CP} , we tried to see if these models can be distinguished by T2HK and DUNE. We have identified the region in the θ_{23} - δ_{CP} parameter space for which Model-A cannot be separated from Model-B in T2HK and DUNE.

In summary, our results demonstrated the capability of T2HK, DUNE, and JUNO to constrain a set of theoretical models based on modular symmetry for which it is not possible to have sum rules connecting the model parameters and the leptonic mixing parameters. These results will have a significant impact in the future in terms of excluding theoretical models in future experiments.

VII. ACKNOWLEDGEMENT

PM and PP want to thank Prime Minister's Research Fellowship (PMRF) scheme for its financial support. MKB would like to acknowledge Program Management Unit for Human Resources & Institutional Development, Research, and Innovation (PMU-B). This academic position is administered in the framework of the F13 (S4P21) National Post-doctoral/Postgraduate System, contract no. B13F660066. RM would like to acknowledge University of Hyderabad IoE project grant no. RC1-20-012. This work has been in part funded by the Ministry of Science and Education of the Republic of Croatia grant No. KK.01.1.1.01.0001. We gratefully acknowledge the use of the CMSD HPC facility of Univ. of Hyderabad to carry out the computational work.

-
- [1] S. Antusch, P. Huber, S.F. King and T. Schwetz, *Neutrino mixing sum rules and oscillation experiments*, *JHEP* **04** (2007) 060 [[hep-ph/0702286](#)].
 - [2] J. Gehrlein, A. Merle and M. Spinrath, *Predictivity of Neutrino Mass Sum Rules*, *Phys. Rev. D* **94** (2016) 093003 [[arXiv:1606.04965](#)].
 - [3] R.N. Mohapatra and G. Senjanović, *Neutrino mass and spontaneous parity nonconservation*, *Physical Review Letters* **44** (1980) 912.
 - [4] V. Brdar, A.J. Helmboldt, S. Iwamoto and K. Schmitz, *Type-I Seesaw as the Common Origin of Neutrino Mass, Baryon Asymmetry, and the Electroweak Scale*, *Phys. Rev. D* **100** (2019) 075029 [[arXiv:1905.12634](#)].
 - [5] G.C. Branco, J.T. Penedo, P.M.F. Pereira, M.N. Rebelo and J.I. Silva-Marcos, *Type-I Seesaw with eV-Scale Neutrinos*, *JHEP* **07** (2020) 164 [[arXiv:1912.05875](#)].
 - [6] S. Bilenky, *Introduction to the physics of massive and mixed neutrinos*, vol. 817 (2010), 10.1007/978-3-642-14043-3.
 - [7] P.H. Gu, H. Zhang and S. Zhou, *A Minimal Type II Seesaw Model*, *Phys. Rev. D* **74** (2006) 076002 [[hep-ph/0606302](#)].

- [8] S. Luo and Z.z. Xing, *The Minimal Type-II Seesaw Model and Flavor-dependent Leptogenesis*, *Int. J. Mod. Phys. A* **23** (2008) 3412 [[arXiv:0712.2610](#)].
- [9] S. Antusch and S.F. King, *Type II Leptogenesis and the neutrino mass scale*, *Phys. Lett. B* **597** (2004) 199 [[hep-ph/0405093](#)].
- [10] W. Rodejohann, *Type II seesaw mechanism, deviations from bimaximal neutrino mixing and leptogenesis*, *Phys. Rev. D* **70** (2004) 073010 [[hep-ph/0403236](#)].
- [11] P.H. Gu, *Double type II seesaw mechanism accompanied by Dirac fermionic dark matter*, *Phys. Rev. D* **101** (2020) 015006 [[arXiv:1907.10019](#)].
- [12] J. McDonald, N. Sahu and U. Sarkar, *Type-II Seesaw at Collider, Lepton Asymmetry and Singlet Scalar Dark Matter*, *JCAP* **04** (2008) 037 [[arXiv:0711.4820](#)].
- [13] Y. Liao, J.Y. Liu and G.Z. Ning, *Radiative Neutrino Mass in Type III Seesaw Model*, *Phys. Rev. D* **79** (2009) 073003 [[arXiv:0902.1434](#)].
- [14] E. Ma, *Pathways to naturally small neutrino masses*, *Phys. Rev. Lett.* **81** (1998) 1171 [[hep-ph/9805219](#)].
- [15] R. Foot, H. Lew, X.G. He and G.C. Joshi, *Seesaw Neutrino Masses Induced by a Triplet of Leptons*, *Z. Phys. C* **44** (1989) 441.
- [16] I. Dorsner and P. Fileviez Perez, *Upper Bound on the Mass of the Type III Seesaw Triplet in an $SU(5)$ Model*, *JHEP* **06** (2007) 029 [[hep-ph/0612216](#)].
- [17] R. Franceschini, T. Hambye and A. Strumia, *Type-III see-saw at LHC*, *Phys. Rev. D* **78** (2008) 033002 [[arXiv:0805.1613](#)].
- [18] X.G. He and S. Oh, *Lepton FCNC in Type III Seesaw Model*, *JHEP* **09** (2009) 027 [[arXiv:0902.4082](#)].
- [19] E. Ma, *Deciphering the Seesaw Nature of Neutrino Mass from Unitarity Violation*, *Mod. Phys. Lett. A* **24** (2009) 2161 [[arXiv:0904.1580](#)].
- [20] M. Hirsch, S. Morisi and J.W.F. Valle, *A_4 -based tri-bimaximal mixing within inverse and linear seesaw schemes*, *Phys. Lett. B* **679** (2009) 454 [[arXiv:0905.3056](#)].
- [21] P.H. Gu and U. Sarkar, *Leptogenesis with Linear, Inverse or Double Seesaw*, *Phys. Lett. B* **694** (2011) 226 [[arXiv:1007.2323](#)].
- [22] A. Das and N. Okada, *Inverse seesaw neutrino signatures at the LHC and ILC*, *Phys. Rev. D* **88** (2013) 113001 [[arXiv:1207.3734](#)].
- [23] E. Arganda, M.J. Herrero, X. Marcano and C. Weiland, *Imprints of massive inverse seesaw model neutrinos in lepton flavor violating Higgs boson decays*, *Phys. Rev. D* **91** (2015) 015001 [[arXiv:1405.4300](#)].
- [24] E. Ma and R. Srivastava, *Dirac or inverse seesaw neutrino masses from gauged $B^\sim L$ symmetry*, *Mod. Phys. Lett. A* **30** (2015) 1530020 [[arXiv:1504.00111](#)].
- [25] A.G. Dias, C.A. de S. Pires, P.S. Rodrigues da Silva and A. Sempieri, *A Simple Realization of the Inverse Seesaw Mechanism*, *Phys. Rev. D* **86** (2012) 035007 [[arXiv:1206.2590](#)].

- [26] A.E. Cárcamo Hernández and S.F. King, *Littlest Inverse Seesaw Model*, *Nucl. Phys. B* **953** (2020) 114950 [[arXiv:1903.02565](#)].
- [27] P.S.B. Dev and A. Pilaftsis, *Minimal Radiative Neutrino Mass Mechanism for Inverse Seesaw Models*, *Phys. Rev. D* **86** (2012) 113001 [[arXiv:1209.4051](#)].
- [28] A.G. Dias, C.A. de S. Pires and P.S.R. da Silva, *How the Inverse See-Saw Mechanism Can Reveal Itself Natural, Canonical and Independent of the Right-Handed Neutrino Mass*, *Phys. Rev. D* **84** (2011) 053011 [[arXiv:1107.0739](#)].
- [29] F. Bazzocchi, *Minimal Dynamical Inverse See Saw*, *Phys. Rev. D* **83** (2011) 093009 [[arXiv:1011.6299](#)].
- [30] P. Panda, P. Mishra, M.K. Behera and R. Mohanta, *Neutrino phenomenology, muon and electron ($g-2$) under $U(1)$ gauged symmetries in an extended inverse seesaw model*, [arXiv:2203.14536](#).
- [31] G.K. Leontaris and N.D. Tracas, *Modular weights, $U(1)$'s and mass matrices*, *Phys. Lett. B* **419** (1998) 206 [[hep-ph/9709510](#)].
- [32] T. Kobayashi, K. Tanaka and T.H. Tatsuishi, *Neutrino mixing from finite modular groups*, *Phys. Rev. D* **98** (2018) 016004 [[arXiv:1803.10391](#)].
- [33] F. Feruglio, *Are neutrino masses modular forms?*, in *From My Vast Repertoire... Guido Altarelli's Legacy*, p. 227. World Scientific, 2019.
- [34] R. de Adelhart Toorop, F. Feruglio and C. Hagedorn, *Finite Modular Groups and Lepton Mixing*, *Nucl. Phys. B* **858** (2012) 437 [[arXiv:1112.1340](#)].
- [35] T.M. Apostol, *The Dedekind eta function*, p. 47. Springer New York, New York, NY, 1990. 10.1007/978-1-4612-0999-73.
- [36] S. Mishra, *Neutrino mixing and Leptogenesis with modular S_3 symmetry in the framework of type III seesaw*, [arXiv:2008.02095](#).
- [37] H. Okada and Y. Orikasa, *Modular S_3 symmetric radiative seesaw model*, *Phys. Rev. D* **100** (2019) 115037 [[arXiv:1907.04716](#)].
- [38] J.T. Penedo and S.T. Petcov, *Lepton Masses and Mixing from Modular S_4 Symmetry*, *Nucl. Phys. B* **939** (2019) 292 [[arXiv:1806.11040](#)].
- [39] P.P. Novichkov, J.T. Penedo, S.T. Petcov and A.V. Titov, *Modular S_4 models of lepton masses and mixing*, *JHEP* **04** (2019) 005 [[arXiv:1811.04933](#)].
- [40] H. Okada and Y. Orikasa, *Neutrino mass model with a modular S_4 symmetry*, [arXiv:1908.08409](#).
- [41] T. Nomura, H. Okada and Y. Shoji, *$SU(4)_C \times SU(2)_L \times U(1)_R$ models with modular A_4 symmetry*, *PTEP* **2023** (2023) 023B04.
- [42] M. Abbas, *Modular A_4 Invariance Model for Lepton Masses and Mixing*, *Phys. Atom. Nucl.* **83** (2020) 764.
- [43] T. Nomura and H. Okada, *Quark and lepton model with flavor specific dark matter and muon $g-2$ in modular A_4 and hidden $U(1)$ symmetries*, [arXiv:2304.13361](#).

- [44] J. Kim and H. Okada, *Fermi-LAT GeV excess and muon $g - 2$ in a modular A_4 symmetry*, [arXiv:2302.09747](#).
- [45] M. Kashav and S. Verma, *On minimal realization of topological Lorentz structures with one-loop seesaw extensions in A_4 modular symmetry*, *JCAP* **03** (2023) 010 [[arXiv:2205.06545](#)].
- [46] K.I. Nagao and H. Okada, *Lepton sector in modular A_4 and gauged $U(1)_R$ symmetry*, *Nucl. Phys. B* **980** (2022) 115841 [[arXiv:2010.03348](#)].
- [47] T. Asaka, Y. Heo and T. Yoshida, *Lepton flavor model with modular A_4 symmetry in large volume limit*, *Phys. Lett. B* **811** (2020) 135956 [[arXiv:2009.12120](#)].
- [48] T. Nomura and H. Okada, *A linear seesaw model with A_4 -modular flavor and local $U(1)_{B-L}$ symmetries*, *JCAP* **09** (2022) 049 [[arXiv:2007.04801](#)].
- [49] H. Okada and Y. Shoji, *A radiative seesaw model with three Higgs doublets in modular A_4 symmetry*, *Nucl. Phys. B* **961** (2020) 115216 [[arXiv:2003.13219](#)].
- [50] M.K. Behera, S. Singirala, S. Mishra and R. Mohanta, *A modular A_4 symmetric scotogenic model for neutrino mass and dark matter*, *J. Phys. G* **49** (2022) 035002 [[arXiv:2009.01806](#)].
- [51] G.J. Ding, S.F. King and X.G. Liu, *Modular A_4 symmetry models of neutrinos and charged leptons*, *JHEP* **09** (2019) 074 [[arXiv:1907.11714](#)].
- [52] G. Altarelli and F. Feruglio, *Tri-bimaximal neutrino mixing, $A(4)$ and the modular symmetry*, *Nucl. Phys. B* **741** (2006) 215 [[hep-ph/0512103](#)].
- [53] M. Kashav and S. Verma, *Broken scaling neutrino mass matrix and leptogenesis based on A_4 modular invariance*, *JHEP* **09** (2021) 100 [[arXiv:2103.07207](#)].
- [54] M.R. Devi, *Retrieving texture zeros in 3+1 active-sterile neutrino framework under the action of A_4 modular-invariants*, [arXiv:2303.04900](#).
- [55] M.K. Singh, S.R. Singh and N.N. Singh, *Modular A_4 symmetry in 3+1 active-sterile neutrino masses and mixings*, [arXiv:2303.10922](#).
- [56] S. Kikuchi, T. Kobayashi, K. Nasu, S. Takada and H. Uchida, *Quark mass hierarchies and CP violation in $A_4 \times A_4 \times A_4$ modular symmetric flavor models*, [arXiv:2302.03326](#).
- [57] S.T. Petcov and M. Tanimoto, *A_4 Modular Flavour Model of Quark Mass Hierarchies close to the Fixed Point $\tau = \omega$* , [arXiv:2212.13336](#).
- [58] M. Abbas and S. Khalil, *Modular A_4 Symmetry With Three-Moduli and Flavor Problem*, [arXiv:2212.10666](#).
- [59] X.K. Du and F. Wang, *Flavor structures of quarks and leptons from flipped $SU(5)$ GUT with A_4 modular flavor symmetry*, *JHEP* **01** (2023) 036 [[arXiv:2209.08796](#)].
- [60] G.J. Ding, S.F. King, J.N. Lu and B.Y. Qu, *Leptogenesis in $SO(10)$ models with A_4 modular symmetry*, *JHEP* **10** (2022) 071 [[arXiv:2206.14675](#)].
- [61] T. Nomura, H. Okada and Y.h. Qi, *Zee model in a modular A_4 symmetry*, [arXiv:2111.10944](#).
- [62] H. Kuranaga, H. Ohki and S. Uemura, *Modular origin of mass hierarchy: Froggatt-Nielsen like mechanism*, *JHEP* **07** (2021) 068 [[arXiv:2105.06237](#)].

- [63] P.P. Novichkov, J.T. Penedo, S.T. Petcov and A.V. Titov, *Modular A_5 symmetry for flavour model building*, *JHEP* **04** (2019) 174 [[arXiv:1812.02158](#)].
- [64] C.Y. Yao, X.G. Liu and G.J. Ding, *Fermion masses and mixing from the double cover and metaplectic cover of the A_5 modular group*, *Phys. Rev. D* **103** (2021) 095013 [[arXiv:2011.03501](#)].
- [65] X.G. Liu and G.J. Ding, *Neutrino Masses and Mixing from Double Covering of Finite Modular Groups*, *JHEP* **08** (2019) 134 [[arXiv:1907.01488](#)].
- [66] P. Mishra, M.K. Behera and R. Mohanta, *Neutrino phenomenology, W mass anomaly & muon $(g - 2)$ in minimal type-III seesaw using T' modular symmetry*, [arXiv:2302.00494](#).
- [67] P. Beneš, H. Okada and Y. Orikasa, *Towards unification of lepton and quark mass matrices from double covering of modular A_4 flavor symmetry*, [arXiv:2212.07245](#).
- [68] H. Okada and Y. Orikasa, *Lepton mass matrix from double covering of A_4 modular flavor symmetry**, *Chin. Phys. C* **46** (2022) 123108 [[arXiv:2206.12629](#)].
- [69] Y. Abe, T. Higaki, J. Kawamura and T. Kobayashi, *Quark and lepton hierarchies from S'_4 modular flavor symmetry*, [arXiv:2302.11183](#).
- [70] Y. Abe, T. Higaki, J. Kawamurab and T. Kobayashi, *Quark masses and CKM hierarchies from S'_4 modular flavor symmetry*, [arXiv:2301.07439](#).
- [71] X. Wang, B. Yu and S. Zhou, *Double covering of the modular A_5 group and lepton flavor mixing in the minimal seesaw model*, *Phys. Rev. D* **103** (2021) 076005 [[arXiv:2010.10159](#)].
- [72] M.K. Behera and R. Mohanta, *Linear Seesaw in A_5' Modular Symmetry With Leptogenesis*, *Front. in Phys.* **10** (2022) 854595 [[arXiv:2201.10429](#)].
- [73] M.K. Behera and R. Mohanta, *Inverse seesaw in A'_5 modular symmetry*, *J. Phys. G* **49** (2022) 045001 [[arXiv:2108.01059](#)].
- [74] HYPER-KAMIOKANDE collaboration, K. Abe et al., *Physics potentials with the second Hyper-Kamiokande detector in Korea*, *PTEP* **2018** (2018) 063C01 [[arXiv:1611.06118](#)].
- [75] DUNE collaboration, B. Abi et al., *Deep Underground Neutrino Experiment (DUNE), Far Detector Technical Design Report, Volume II: DUNE Physics*, [arXiv:2002.03005](#).
- [76] JUNO collaboration, F. An et al., *Neutrino Physics with JUNO*, *J. Phys. G* **43** (2016) 030401 [[arXiv:1507.05613](#)].
- [77] I. Esteban, M.C. Gonzalez-Garcia, M. Maltoni, T. Schwetz and A. Zhou, *The fate of hints: updated global analysis of three-flavor neutrino oscillations*, *JHEP* **09** (2020) 178 [[arXiv:2007.14792](#)].
- [78] M. Blennow, M. Ghosh, T. Ohlsson and A. Titov, *Testing Lepton Flavor Models at ESSnuSB*, *JHEP* **07** (2020) 014 [[arXiv:2004.00017](#)].
- [79] M. Blennow, M. Ghosh, T. Ohlsson and A. Titov, *Probing Lepton Flavor Models at Future Neutrino Experiments*, *Phys. Rev. D* **102** (2020) 115004 [[arXiv:2005.12277](#)].
- [80] S.S. Chatterjee, M. Masud, P. Pasquini and J.W.F. Valle, *Cornering the revamped BMV model with neutrino oscillation data*, *Phys. Lett. B* **774** (2017) 179 [[arXiv:1708.03290](#)].

- [81] S.K. Agarwalla, S.S. Chatterjee, S.T. Petcov and A.V. Titov, *Addressing Neutrino Mixing Models with DUNE and T2HK*, *Eur. Phys. J. C* **78** (2018) 286 [[arXiv:1711.02107](#)].
- [82] P. Ballett, S.F. King, S. Pascoli, N.W. Prouse and T. Wang, *Precision neutrino experiments vs the Littlest Seesaw*, *JHEP* **03** (2017) 110 [[arXiv:1612.01999](#)].
- [83] M.K. Behera, S. Mishra, S. Singirala and R. Mohanta, *Implications of A_4 modular symmetry on neutrino mass, mixing and leptogenesis with linear seesaw*, *Phys. Dark Univ.* **36** (2022) 101027 [[arXiv:2007.00545](#)].
- [84] S. Dawson, *Electroweak Symmetry Breaking and Effective Field Theory*, in *Theoretical Advanced Study Institute in Elementary Particle Physics: Anticipating the Next Discoveries in Particle Physics*, p. 1, 12, 2017, [arXiv:1712.07232](#), DOI.
- [85] PARTICLE DATA GROUP collaboration, P. Zyla et al., *Review of Particle Physics*, *PTEP* **2020** (2020) 083C01.
- [86] P. Mishra, M.K. Behera, P. Panda and R. Mohanta, *Type III seesaw under A_4 modular symmetry with leptogenesis*, *Eur. Phys. J. C* **82** (2022) 1115 [[arXiv:2204.08338](#)].
- [87] NuFIT-5.2, *Nufit*, [www.nu-fit.org](#), 2022.
- [88] K.A. Hochmuth, S.T. Petcov and W. Rodejohann, $U(PMNS) = U^{**\dagger}(l) U(\nu)$, *Phys. Lett. B* **654** (2007) 177 [[arXiv:0706.2975](#)].
- [89] PLANCK collaboration, N. Aghanim et al., *Planck 2018 results. VI. Cosmological parameters*, *Astron. Astrophys.* **641** (2020) A6 [[arXiv:1807.06209](#)].
- [90] S. Vagnozzi, E. Giusarma, O. Mena, K. Freese, M. Gerbino, S. Ho et al., *Unveiling ν secrets with cosmological data: neutrino masses and mass hierarchy*, *Phys. Rev. D* **96** (2017) 123503 [[arXiv:1701.08172](#)].
- [91] S. Roy Choudhury and S. Choubey, *Updated Bounds on Sum of Neutrino Masses in Various Cosmological Scenarios*, *JCAP* **09** (2018) 017 [[arXiv:1806.10832](#)].
- [92] B. Roe, *Chi-square Fitting When Overall Normalization is a Fit Parameter*, [arXiv:1506.09077](#).
- [93] G.J. Ding, S.F. King and J.N. Lu, *$SO(10)$ models with A_4 modular symmetry*, *JHEP* **11** (2021) 007 [[arXiv:2108.09655](#)].
- [94] P. Huber, M. Lindner and W. Winter, *Simulation of long-baseline neutrino oscillation experiments with GLoBES (General Long Baseline Experiment Simulator)*, *Comput. Phys. Commun.* **167** (2005) 195 [[hep-ph/0407333](#)].
- [95] P. Huber, J. Kopp, M. Lindner, M. Rolinec and W. Winter, *New features in the simulation of neutrino oscillation experiments with GLoBES 3.0: General Long Baseline Experiment Simulator*, *Comput. Phys. Commun.* **177** (2007) 432 [[hep-ph/0701187](#)].
- [96] DUNE collaboration, B. Abi et al., *Experiment Simulation Configurations Approximating DUNE TDR*, [arXiv:2103.04797](#).